

Potential for low-cost carbon dioxide removal through tropical reforestation

Jonah Busch^{1*}, Jens Engelmann², Susan C. Cook-Patton³, Bronson W. Griscom³, Timm Kroeger³, Hugh Possingham³ and Priya Shyamsundar³

Achieving the 1.5–2.0°C temperature targets of the Paris climate agreement requires not only reducing emissions of greenhouse gases (GHGs) but also increasing removals of GHGs from the atmosphere^{1,2}. Reforestation is a potentially large-scale method for removing CO₂ and storing it in the biomass and soils of ecosystems^{3–8}, yet its cost per tonne remains uncertain^{6,9}. Here, we produce spatially disaggregated marginal abatement cost curves for tropical reforestation by simulating the effects of payments for increased CO₂ removals on land-cover change in 90 countries. We estimate that removals from tropical reforestation between 2020–2050 could be increased by 5.7 GtCO₂ (5.6%) at a carbon price of US\$20 tCO₂⁻¹, or by 15.1 GtCO₂ (14.8%) at US\$50 tCO₂⁻¹. Ten countries comprise 55% of potential low-cost abatement from tropical reforestation. Avoided deforestation offers 7.2–9.6 times as much potential low-cost abatement as reforestation overall (55.1 GtCO₂ at US\$20 tCO₂⁻¹ or 108.3 GtCO₂ at US\$50 tCO₂⁻¹), but reforestation offers more potential low-cost abatement than avoided deforestation at US\$20 tCO₂⁻¹ in 21 countries, 17 of which are in Africa.

There is a lack of spatially disaggregated marginal abatement cost (MAC) curves for tropical reforestation; that is, estimates of how much CO₂ could be removed from the atmosphere through reforestation at various costs-per-tonne at particular places and times¹⁰. Analyses of the cost per tonne of removing CO₂ through tropical reforestation have been limited to site-specific case studies¹¹ and aggregate sectoral estimates⁹. By contrast, multiple MAC curves (reviewed in ref. ¹²) have estimated that avoided tropical deforestation could abate 0.8–4.4 billion metric tonnes of CO₂ (GtCO₂yr⁻¹) in 2020 at a cost of US\$20 tCO₂⁻¹.

Generating a MAC curve for reforestation is more challenging than for avoided deforestation for several reasons. First, historical reforestation is harder to observe than deforestation because it happens gradually. Second, accounting for the trajectory of CO₂ removal (that is, sequestration) over time from reforestation is complicated compared to carbon loss from deforestation because it is subject to reversals due to harvest or natural losses. Third, different types of forest growth (for example natural forests; plantations) have different carbon removal trajectories.

Newly available data let us address all three of these challenges. For the first challenge, a dataset that measures global forest cover consistently in 2000 and 2010 (ref. ¹³, based on ref. ¹⁴) provides the best assessment yet of pantropical forest-cover gain. For the second challenge, a database of carbon stocks in secondary forests and plantations at different ages¹⁵ lets us model carbon removal trajectories for both secondary natural forests and plantations across the

tropics. And for the third challenge, a dataset of the location of plantations in seven tropical countries¹⁶ lets us differentiate reforestation with secondary natural forests from reforestation with plantations.

Here we use a gridded dynamic land-cover-change model to produce pantropical, spatially disaggregated MAC curves for reforestation; that is, the transition of non-forested lands to forests through both natural regrowth and plantations. We simulate the effect of payments for increased carbon removals on future land-cover changes, accounting for site characteristics including slope, elevation, distance from cities, protected status, initial forest cover, agricultural revenue potential, continent and biome. Our estimates represent economic potentials subject to the modelling assumption that land users would be as responsive to changes in carbon prices as they were to historical variation in agricultural prices; these estimates do not account for economic, social, legal or technical hurdles associated with operationalizing carbon price incentives under specific policies. We geographically disaggregate the cost per tonne of carbon removals from reforestation, identifying countries and regions with the greatest low-cost abatement potential. We also produce MAC curves for reducing emissions from tropical deforestation using identical methods, which enables a direct comparison of the relative cost per tonne of reforestation and avoided deforestation pantropically for 90 countries.

From 2000 to 2010, 94.0 million hectares (Mha) of tropical land were reforested; that is, transitioned from non-forest to forest at a 30% tree-cover threshold (ref. ¹³, based on ref. ¹⁴). Using carbon removal factors that we constructed for this paper (Supplementary Figs. 1 and 2), this corresponds to 9.5 GtCO₂ removed from reforestation from 2000 to 2010. The areas reforested between 2000 and 2010 would be expected to remove an additional 21.8 GtCO₂ from 2010 to 2050 if they remain forested, and the country-specific share of reforestation that is secondary natural forest—rather than cyclically harvested plantation—remains stable. Our estimates are smaller than previous estimates of 4.3–6.2 GtCO₂yr⁻¹ removed over the decade^{17–19}, because those estimates also included removals from reforestation that occurred before 2000, and regrowth of degraded forests.

From 2000 to 2010, 139.1 Mha of tropical land were deforested; that is, transitioned from forest to non-forest at a 30% tree-cover threshold (ref. ¹³, based on ref. ¹⁴), which produced 49.4 GtCO₂ emissions. This is consistent with previous estimates of 2.3–10.3 GtCO₂yr⁻¹ of emissions from deforestation during the first decade of the 2000s (summarized in ref. ¹²).

Determinants of pantropical forest-cover changes from 2000–2010 were largely as expected (Supplementary Table 5). Reforestation was significantly greater on land that was flatter, at lower elevation,

¹Earth Innovation Institute, San Francisco, CA, USA. ²Department of Agricultural and Applied Economics, University of Wisconsin, Madison, WI, USA.

³The Nature Conservancy, Arlington, VA, USA. *e-mail: jbusch@earthinnovation.org

inside protected areas and with lower potential agricultural revenue. Deforestation was significantly greater on land that was closer to cities, flatter, outside protected areas and with greater potential agricultural revenue. These results are broadly consistent with the findings of a meta-analysis of determinants of deforestation and reforestation²⁰. Reforestation was highest at low–intermediate levels of forest cover, whereas deforestation was highest at intermediate–high levels of forest cover (Supplementary Fig. 3). Reforestation was higher in Africa and lower in Latin America, whereas deforestation was higher in Asia and lower in Africa. Determinants of reforestation varied across the continents (Supplementary Table 6).

We projected 387.8 Mha of reforestation and 541.5 Mha of deforestation from 2020 to 2050 under a business-as-usual scenario (BAU; Supplementary Fig. 4). These projected land-cover changes correspond to 102.5 GtCO₂ removals from reforestation, and 256.9 GtCO₂ emissions from deforestation from 2020 to 2050 under a BAU scenario (Supplementary Fig. 5).

A carbon price of US\$20 tCO₂⁻¹ would incentivize tropical land users to increase reforestation by 31.8 Mha (8.2%) to 419.6 Mha, and reduce deforestation by 70.9 Mha (13.1%) to 470.6 Mha from 2020 to 2050 relative to a BAU scenario (Supplementary Fig. 6). This corresponds to increasing removals from reforestation by 5.7 GtCO₂ (5.6%) to 108.3 GtCO₂, and reducing emissions from deforestation by 55.1 GtCO₂ (21.5%) to 201.7 GtCO₂ from 2020 to 2050 (Supplementary Fig. 7). A carbon price of US\$50 tCO₂⁻¹ would increase reforestation by 84.1 Mha (21.7%) to 471.9 Mha, and reduce deforestation by 149.7 Mha (27.6%) to 391.8 Mha from 2020 to 2050 (Supplementary Fig. 6). This corresponds to increasing removals from reforestation by 15.1 GtCO₂ (14.8%) to 117.7 GtCO₂, and reducing emissions from deforestation by 108.3 GtCO₂ (42.2%) to 148.5 GtCO₂ from 2020 to 2050 (Supplementary Fig. 7).

The potential for low-cost abatement increases over time for both increased removals and reduced emissions; that is, MAC curves shift outwards in later decades (Fig. 1). Increased removals from reforestation at US\$20 tCO₂⁻¹ are 101% higher in 2030–2040 and 188% higher in 2040–2050 than in 2020–2030, while reduced emissions from deforestation at US\$20 tCO₂⁻¹ are 32% higher in 2030–2040 and 74% higher in 2040–2050 than in 2020–2030. The potential low-cost abatement increases because projected reforestation and deforestation both increase under a BAU scenario, and because reforestation in early periods continues to remove carbon in later periods as secondary forests regrow.

Latin America comprised 40% of low-cost removals from reforestation between 2020 and 2050 at US \$20 tCO₂⁻¹, followed by Africa (36%) and Asia (24%). Latin America also comprised 48% of low-cost reductions in emissions from deforestation, followed by Asia (29%) and Africa (23%).

The top ten countries for increased removals from tropical reforestation between 2020 and 2050 at US \$20 t⁻¹ (representing 55% of total removals) were Brazil (tropical), Indonesia, the Democratic Republic of the Congo, Mexico (tropical), Angola, Colombia, India (tropical), Tanzania, Mozambique (tropical) and Thailand (Supplementary Table 7). The top ten countries for reducing emissions from deforestation between 2020 and 2050 at US\$20 tCO₂⁻¹ were Brazil (tropical), Indonesia, the Democratic Republic of the Congo, Peru, Colombia, Bolivia, Papua New Guinea, Republic of Congo, Venezuela and Malaysia.

The potential to increase removals and reduce emissions at low cost varied across countries (Fig. 2). In more than three-quarters of countries ($n=69$, of a total of 90), increased removals from reforestation were lower than reduced emissions from deforestation at US\$20 tCO₂⁻¹ (Fig. 3). Of the 21 countries with greater potential for increasing removals than reducing emissions at US\$20 tCO₂⁻¹, 17 were in Africa.

Our results had varying sensitivity to alternative data, parameter choices and modelling decisions (Supplementary Table 8). Results

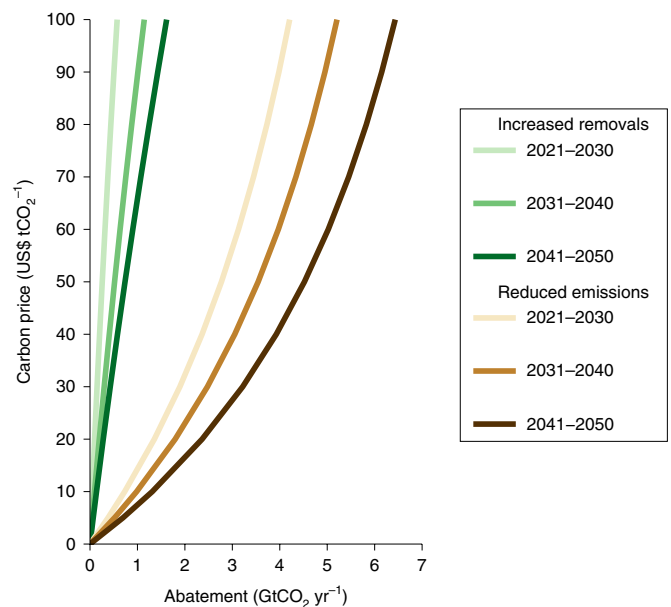


Fig. 1 | Global MAC curves. The potential CO₂ abatement from tropical reforestation and reduced emissions from tropical deforestation is shown for decades from 2020 to 2050.

for increased removals from 2020 to 2050 at US\$20 tCO₂⁻¹ were most sensitive (>40% difference relative to the base scenario) to the tree-cover threshold used to define forest-cover change, assumptions about future agricultural prices and the salience of carbon price versus agricultural price in land-cover decisions. We discuss sensitivities and caveats in detail in the Supplementary Information.

We have produced pantropical, spatially explicit estimates of the cost per tonne of CO₂ abatement through reforestation (that is, MAC curves). Using our pantropical, spatially explicit MAC curves, we estimate that 5.7 GtCO₂ of CO₂ removal from reforestation is available between 2020–2050 at US\$20 tCO₂⁻¹, whereas 15.1 GtCO₂ is available at US\$50 tCO₂⁻¹. On an annualized basis, these potentials are respectively equivalent to 0.4% and 1.1% of global greenhouse gas (GHG) emissions excluding land-use change and forestry in 2014 (ref. ²¹).

The amount of abatement available from reducing emissions from deforestation at US\$20–50 tCO₂⁻¹ is 7.2–9.6 greater than from increasing removals from reforestation. This disparity is due to slower carbon removal through reforestation than emissions from deforestation, especially on soils and in peat forests. On a decadal-average basis, the combined potential of increasing removals from reforestation and reducing emissions from deforestation at US\$20–50 tCO₂⁻¹ is equivalent to 10.3–20.9% of emission reductions needed from 2020–2030 for a >66% chance of holding global warming below 2 °C (ref. ⁵). Although avoiding deforestation is a more efficient way to mitigate climate change than increasing reforestation overall, both can and should be done where cost effective.

Regions vary in the relative importance of reforestation and avoided deforestation for mitigating climate change. Latin America is the region with the most low-cost potential for both increased removals from reforestation and reduced emissions from deforestation. However, Africa is the region with the second-most low-cost abatement reforestation, whereas Asia is the region with the second-lowest-cost abatement potential from avoided deforestation.

Our estimates of cost-effective potential abatement are more conservative than previous non-spatial studies. Our estimates that tropical reforestation could remove 0.072–0.86 GtCO₂ yr⁻¹

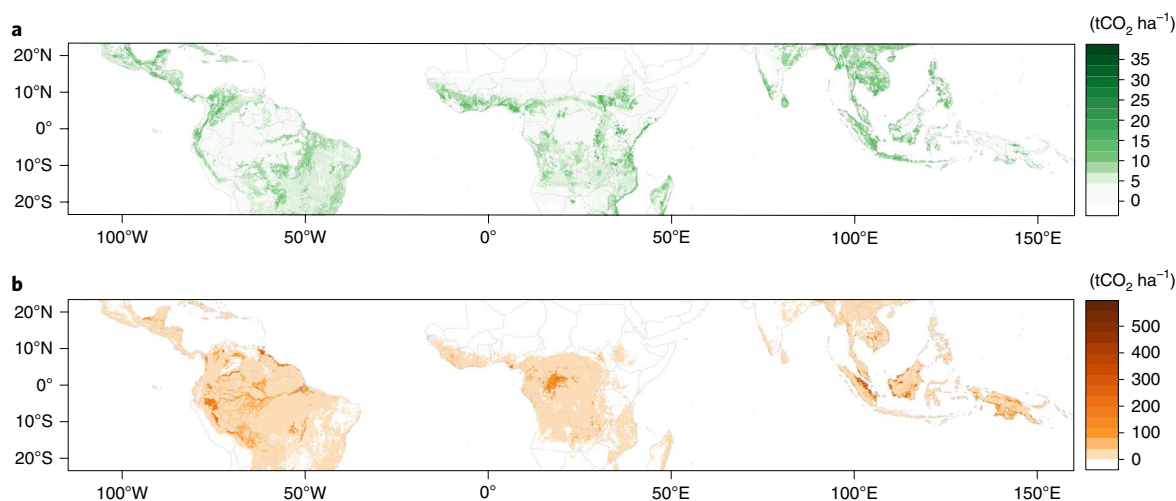


Fig. 2 | Maps of increased removals from reforestation and reduced emissions from deforestation at a carbon price of US\$20 tCO₂⁻¹ from 2020 to 2050. **a**, Increased removals from reforestation. **b**, Reduced emissions from deforestation.

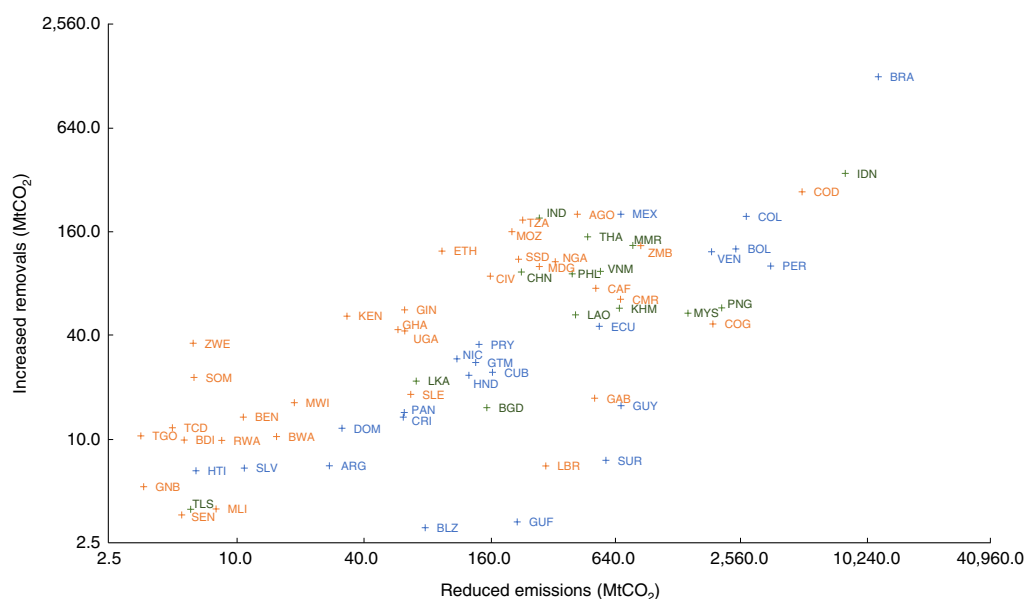


Fig. 3 | Increased removals from tropical reforestation and reduced emissions from deforestation in 77 countries at US\$20 tCO₂⁻¹ from 2020 to 2050. Countries with less than 2.5 MtCO₂ in either mitigation option are not shown ($n=13$). Axes are log-scale for presentation. Blue data are for Latin America/Caribbean; orange data are for Africa; and green data are for Asia. The dashed line is a 1:1 line. The three-letter country codes are from the UN Trade Statistics (<https://unstats.un.org/unsd/tradekb/knowledgebase/country-code>) and are listed in Supplementary Table 7.

at US\$10–100 tCO₂⁻¹ in 2030 were lower at high prices than the 0–3.04 GtCO₂ yr⁻¹ at US\$10–100 tCO₂⁻¹ in 2030 estimated in ref. ⁵. Our estimates that tropical reforestation could remove 0.078, 0.49, 0.84, and 1.84 GtCO₂ yr⁻¹ at US\$5, US\$30, US\$50 and US\$100 tCO₂⁻¹ in 2050 were also lower than the 0.5–3.6 GtCO₂ yr⁻¹ at US\$5–50 tCO₂⁻¹ in 2050 that was estimated in ref. ⁶ for afforestation and reforestation globally. Multiple differences between our study and previous studies might contribute to our lower estimates of cost-effective potential abatement. These include higher estimated economic returns to agricultural land competing with forests; less land available for reforestation and afforestation; slower estimated carbon accumulation rates following reforestation; and MAC curves constructed from econometric relationships between pantropical data on agricultural potential and land-cover change rather than extrapolated from a small number of case studies.

Relative to the other negative emissions technologies reviewed in ref. ⁶, we estimate that tropical reforestation has greater cost-effective abatement potential in 2050 than bio-energy with carbon capture and storage (BECCS) (0.5–5 GtCO₂ yr⁻¹ at US\$100–200 tCO₂⁻¹) and direct air carbon capture and storage (0.5–5 GtCO₂ yr⁻¹ at US\$100–300 tCO₂⁻¹); comparable cost-effective abatement potential in 2050 to biochar (0.5–2 GtCO₂ yr⁻¹ at US\$30–120 tCO₂⁻¹); and less cost-effective abatement potential in 2050 than enhanced weathering (2–4 GtCO₂ yr⁻¹ at US\$50–200 tCO₂⁻¹) and soil carbon sequestration (2–5 GtCO₂ yr⁻¹ at US\$0–100 tCO₂⁻¹). Estimates of costs and potentials for other negative emissions technologies remain highly uncertain and would benefit from future research.

Tropical reforestation can contribute to cost-effectively mitigating climate change. Indeed, countries have included more than 120 Mha of reforestation in their national climate pledges²², with

forest-based mitigation comprising one-quarter of emission reductions planned by countries²³. However, reforestation programmes are constrained by economic, social, legal and technical challenges (see refs. ^{24,25}) and sensitivity to biological diversity safeguards²⁶. Site-level efforts to operationalize carbon price incentives for reforestation such as the Clean Development Mechanism have been hampered by the need to address carbon accounting concerns related to leakage, additionality and permanence²⁷. In principle, such concerns can be eased by country- or jurisdiction-level carbon accounting for Reducing Emissions from Deforestation and Forest Degradation plus enhancing forest carbon stocks (REDD+). Most REDD+ finance so far has concentrated on reduced emissions from deforestation due to the relatively advanced monitoring capabilities for this activity²⁸. Rapid improvements in monitoring of removals from reforestation could advance the use of carbon price incentives for reforestation as well.

Online content

Any methods, additional references, Nature Research reporting summaries, source data, statements of code and data availability and associated accession codes are available at <https://doi.org/10.1038/s41558-019-0485-x>.

Received: 13 August 2018; Accepted: 23 April 2019;

Published online: 27 May 2019

References

- Minx, J. C. et al. Negative emissions—Part 1: research landscape and synthesis. *Environ. Res. Lett.* **13**, 063001 (2018).
- Rogelj, J. et al. in *Global Warming of 1.5°C*. (eds Masson-Delmotte, V. et al.) Ch. 2 (IPCC, Cambridge Univ. Press, 2018).
- Dixon, R. K. et al. Carbon pools and flux of global forest ecosystems. *Science* **263**, 185–191 (1994).
- Silver, W. L., Ostertag, R. & Lugo, A. E. The potential for carbon sequestration through reforestation of abandoned tropical agricultural and pasture lands. *Restor. Ecol.* **8**, 394–407 (2000).
- Griscom, B. et al. Natural climate solutions. *Proc. Natl Acad. Sci. USA* **114**, 11645–11650 (2017).
- Fuss, S. et al. Negative emissions—Part 2: costs, potentials and side effects. *Environ. Res. Lett.* **13**, 063002 (2018).
- Hawes, M. Planting carbon storage. *Nat. Clim. Change* **8**, 556–558 (2018).
- Mitchard, E. The tropical forest carbon cycle and climate change. *Nature* **559**, 527–534 (2018).
- Smith, et al. in *Climate Change 2014: Impacts, Adaptation, and Vulnerability* (eds Field, C. B. et al.) Ch. 11 (IPCC, Cambridge Univ. Press, 2014).
- Kesicki, F. & Strachan, N. Marginal abatement cost (MAC) curves: confronting theory and practice. *Environ. Sci. Policy* **14**, 1195–1204 (2011).
- Gilroy, J. J. et al. Cheap carbon and biodiversity co-benefits from forest regeneration in a hotspot of endemism. *Nat. Clim. Change* **4**, 503–507 (2014).
- Busch, J. & Engelmann, J. Cost-effectiveness of reducing emissions from tropical deforestation, 2016–2050. *Environ. Res. Lett.* **13**, 015001 (2018).
- Global Tree Canopy Cover Circa 2010* (United States Geological Survey, accessed 12 April 2018).
- Hansen, M. C. et al. High-resolution global maps of 21st-century forest cover change. *Science* **42**, 850–853 (2013).
- Anderson-Teixeira, K. J., Wang, M. M. H., McGarvey, J. C. & LeBauer, D. S. Carbon dynamics of mature and regrowth tropical forests derived from a pantropical database (TropForC-db). *Glob. Change Biol.* **22**, 1690–1709 (2016).
- Petersen, R. et al. *Mapping Tree Plantations with Multispectral Imagery: Preliminary Results for Seven Tropical Countries* (World Resources Institute, 2016).
- Pan, Y. et al. A large and persistent carbon sink in the world's forests. *Science* **333**, 988–993 (2011).
- Baccini, A. et al. Estimated carbon dioxide emissions from tropical deforestation improved by carbon-density maps. *Nat. Clim. Change* **2**, 182–185 (2012).
- Grace, J. et al. Perturbations in the carbon budget of the tropics. *Glob. Change Biol.* **20**, 3238–3255 (2014).
- Busch, J. & Ferretti-Gallon, K. What drives deforestation and what stops it? A meta-analysis. *Rev. Environ. Econ. Policy* **11**, 3–23 (2017).
- CAIT *Climate Data Explorer* (World Resources Institute, accessed 15 June 2018).
- Progress on the New York Declaration on Forests—An Assessment Framework and Initial Report* (Climate Focus, 2015).
- Grassi, G. et al. The key role of forests in meeting climate targets requires science for credible mitigation. *Nat. Clim. Change* **7**, 220–228 (2017).
- Chomitz, K. M., Brenes, E. & Constantino, L. Financing environmental services: the Costa Rican experience and its implications. *Sci. Total Environ.* **240**, 157–169 (1999).
- Chazdon, R. L. & Guariguata, M. R. Natural regeneration as a tool for large-scale forest restoration in the tropics: prospects and challenges. *Biotropica* **48**, 716–730 (2016).
- Veldman, J. W. et al. Where tree planting and forest expansion are bad for biodiversity and ecosystem services. *Bioscience* **65**, 1011–1017 (2015).
- Thomas, S., Dargusch, P., Harrison, S. & Herbohn, J. Why are there so few afforestation and reforestation clean development projects? *Land Use Policy* **27**, 880–887 (2010).
- Goetz, S. et al. Measurement and monitoring needs, capabilities and potential for addressing reduced emissions from deforestation and forest degradation under REDD+. *Environ. Res. Lett.* **10**, 123001 (2015).

Acknowledgements

We acknowledge the generous support of an anonymous individual donor and the Norwegian Agency for Development Cooperation (QZA-0701 QZA-16/0162).

Author contributions

J.B. and P.S. planned the project. J.B., J.E., and S.C.C.-P. prepared and analysed data. J.B., J.E., S.C.C.-P., B.W.G., T.K., H.P. and P.S. contributed to writing the paper.

Competing interests

The authors declare no competing interests.

Additional information

Supplementary information is available for this paper at <https://doi.org/10.1038/s41558-019-0485-x>.

Reprints and permissions information is available at www.nature.com/reprints.

Correspondence and requests for materials should be addressed to J.B.

Peer review information: *Nature Climate Change* thanks Helal Ahammad, Antonio Trabucco and the other, anonymous, reviewer(s) for their contribution to the peer review of this work.

Publisher's note: Springer Nature remains neutral with regard to jurisdictional claims in published maps and institutional affiliations.

© The Author(s), under exclusive licence to Springer Nature Limited 2019

Methods

Overview of methods. We produced MAC curves for tropical reforestation and avoided deforestation using a top-down approach, which assumes that mitigation is partly a response of human behaviour to economic forces, and uses large-scale modelling to simulate the aggregate response of abatement suppliers to a variable carbon price. This contrasts with a bottom-up approach, which accounts for costs on the basis of detailed local or project-specific data, but which is difficult to undertake across many geographies or technologies¹⁰.

We generated MAC curves by simulating the effects of hypothetical carbon payments on reforestation and deforestation, extending the approach used in refs. ^{12,29,30}. First, we constructed a pantropical land-cover-change model to estimate the responsiveness of observed reforestation and deforestation to variation in global agricultural prices, while controlling for other economic and physical determinants of land-cover change. Next, we projected reforestation and deforestation in future decades, assuming that there will be no changes in agro-ecological, economic and policy conditions that affect land-cover change (that is, a BAU scenario). We projected the share of reforestation that would occur as secondary natural forests versus plantations on the basis of historical data on the location of plantations in seven countries. Using a database of aboveground biomass in stands across the tropics (Supplementary Fig. 1), we then constructed new carbon removal trajectories in aboveground biomass. We used these trajectories to convert our projections of reforestation and deforestation into carbon removals and emissions in aboveground biomass, belowground biomass and peat and non-peat soils. We then projected removals from reforestation, and emissions from deforestation, at varying carbon prices, assuming land-use decision makers would be as responsive to future changes in carbon prices as they were to historical variation in agricultural prices. We used our estimates of carbon removed or emitted at different carbon prices to trace MAC curves. Finally, we analysed the sensitivity of our results to key data sources, parameter assumptions and modelling decisions.

Land-cover-change model. We used a pantropical land-cover-change model to estimate how historical reforestation and deforestation varied in response to agricultural prices, while controlling for other factors that influence land-cover change.

The primary dependent variable in our land-cover-change model, reforestation, was constructed from data on forest cover in 2000 and 2010¹³. These data were derived from 30-m Landsat satellite measurements using spatially consistent methods¹⁴. The dataset replicated tree cover for 2010 by using the same methods used in ref. ¹⁴ in 2000. The globally consistent algorithm used in the data¹⁴ means they may (for example, ref. ³¹) or may not (for example, ref. ³²) be as accurate in some regions as locally calibrated data. We classified tree cover into forest and non-forest by applying a tree-cover threshold of 30%, which is the high end of the range (10–30%) of the UNFCCC's forest definition³³. The use of alternative tree-cover thresholds of 10% and 50% in sensitivity analyses resulted in large (76% and 65% respectively) falls in increased removals from reforestation at US\$20 tCO₂⁻¹ relative to the base scenario with a tree-cover threshold of 30%. We defined all transitions from non-forest in 2000 to forest in 2010 as 'reforestation', as our data did not distinguish between the changes that occurred due to anthropogenic versus natural processes. This definition is inclusive of afforestation³³, however, we avoid using the term as it can suggest intentional conversion of native non-forest ecosystems to exotic tree cover, an activity that we do not endorse as it would violate biodiversity safeguards²⁶. Similarly, we defined all transitions from forest in 2000 to non-forest in 2010 as 'deforestation', without distinguishing between anthropogenic or natural processes. In a sensitivity analysis, we removed forest areas identified as oil palm plantations from reforestation and deforestation, which resulted in a small (3%) decrease in increased removals from reforestation at US\$20 tCO₂⁻¹ relative to the base scenario in which oil palm plantations were not removed. Summary statistics for reforestation, deforestation and other variables by continent are shown in Supplementary Table 1.

The main independent variable in our land-cover-change model was maximum potential gross agricultural revenue. We constructed the agricultural revenue data by selecting the maximum product of potential crop yield across 21 crop types on the basis of global agro-ecological zones³⁴ and the production-weighted average of national farmgate prices³⁵ for the top five producer countries of each crop in the decade 2000–2010, following refs. ^{36,12}. We assumed 30 yr of agricultural revenues discounted at 10% annually; a rate that is typically used by development banks for evaluating public investments in developing countries³⁷, and that is consistent with private decision-making in the developing world³⁸. The use of higher (15%) and lower (3%; 7%) discount rates in a sensitivity analysis resulted in small to moderate (8–19%) differences in increased removals from reforestation at US\$20 tCO₂⁻¹ relative to the base scenario with a 10% discount rate. The potential agricultural revenue variable assumes that farmers maximize yields, face global prices and produce crops that reflect agro-ecological conditions.

As control variables in our land-cover-change model, we included data on other widely confirmed determinants of forest-cover change³⁰, including slope and elevation³⁹, Euclidean distance from the nearest city of more than 750,000 people in the same country in the year 2010⁴⁰ and strict and multiple-use protected areas⁴¹, as well as the biome type⁴², which could influence rates of forest recovery. We included continental dummy variables to account for systematic differences

in deforestation rates across Latin America/Caribbean, sub-Saharan Africa and tropical Asia. In a sensitivity analysis, we replaced fixed effects for the biome and continent with fixed effects for ecoregions⁴² and countries to control for more granular institutional and biological factors. This resulted in a moderate (37%) fall in increased removals from reforestation at US\$20 tCO₂⁻¹ relative to the base scenario with continent and biome fixed effects. In a sensitivity analysis, we applied three continent-specific models, which resulted in a small (5%) rise in increased removals from reforestation at US\$20 tCO₂⁻¹ relative to the base scenario using a single pantropical model.

We also included four terms representing a fourth-order polynomial on initial forest cover (that is, forest cover, forest-cover squared and so on) as control variables to capture nonlinear trends in land-cover change across forest cover; for example, the inverted-U-shaped relationship between forest cover and deforestation at the cell level that was found in ref. ¹². In sensitivity analyses, we attempted to control for timber prices using the average export value per cubic metre of industrial non-coniferous tropical roundwood⁴³, which resulted in a small (2%) rise in increased removals from reforestation at US\$20 tCO₂⁻¹ relative to the base scenario without this variable. Globally consistent data on road coverage, an important determinant of deforestation, were not available (see ref. ⁴⁴). We also excluded revenue from cattle, an important driver of deforestation in Latin America (for example, ref. ⁴⁵), for which no globally consistent maps of potential production were available.

We aggregated all data into 0.05° grid cells (~5.5 km wide at the Equator) following ref. ¹². By aggregating spatial data to relatively coarse grid-cell sizes, we were able to capture the full wall-to-wall spatial variation in forest cover change within a manageable number of cells, with the trade-off of losing fine-scale spatial specificity. Using coarser-resolution cells had the added benefits of diluting the effects of possible spatial misalignments between datasets, which enabled easier interpolation of missing data within cells (for example, for forest carbon density), and subsumed localized spatial autocorrelation. Residual spatial autocorrelation at larger scales may result in downward-biased standard errors; this is less of a concern for numerical modelling than for hypothesis testing.

We limited the scope to the tropics (as defined in ref. ¹⁸, following ref. ¹²), which contained 1,829,516 of the 5.5 × 5.5 km² grid cells. We excluded the desert and mangrove biomes⁴² from the scope of the analysis, as these biomes had too few observations in the reforestation biomass database described below¹⁵ to produce reliable carbon removal trajectories. Carbon removal trajectories for mangrove forests, as well as soils and peatlands, would benefit from future research. We further excluded all grid cells that had zero forest cover in both 2000 and 2010, under the assumption that such lands are not biophysically suitable for reforestation (for example mountain tops; savannahs; urban areas), regardless of the biome type identified in ref. ⁴². The exclusion of 235,403 grid cells resulted in a dataset that contained 1,594,113 grid cells in 90 countries.

We modelled historical reforestation as a function of economic and biophysical driver variables. We used a Poisson quasi-maximum likelihood estimator⁴⁶ in the same way as in previous analyses of grid-cell-level forest cover change (for example, refs. ^{12,30,47}). The Poisson quasi-maximum likelihood estimator functional form is theoretically consistent with forest-cover loss or gain within a 5.5 × 5.5 km² grid cell being the count of many independent, discrete binary observations of forest cover loss or gain at the level of 30 × 30 m² remote sensing data. We tested the use of alternative functional forms (that is, Tweedie; negative binomial) in sensitivity analyses, which resulted in small (0–9%) differences in increased removals from reforestation at US\$20 tCO₂⁻¹ relative to the base scenario using the Poisson quasi-maximum likelihood estimator.

The regression model was:

$$R_i = \exp(\beta_0^r + \beta_1^r AG_i + \mathbf{X}_i^r \beta_2^r + \mathbf{F}_i^r \beta_3^r + \gamma_i^r + \mu_i^r + \epsilon_i^r) \quad (1)$$

Here, the dependent variable, R_i , is the fraction of the area of cell i that underwent a non-forest to forest transition from 2000 to 2010. Independent variables include the net present value of maximum potential agricultural revenue (AG_i); a vector of slope, elevation, distance from the nearest city of more than 750,000 people, fraction of a cell within strict protected areas and fraction of a cell within multiple-use protected areas (\mathbf{X}_i); and a fourth-order polynomial on forest cover as a fraction of a cell (\mathbf{F}_i). The γ_i and μ_i terms are fixed effects for the continent and biome respectively; in a sensitivity analysis, we applied fixed effects for countries and ecoregions instead, as described above. The superscript r denotes reforestation, ϵ_i is an error term and β terms are regression coefficients. A full list of variables and parameters used in the model is shown in Supplementary Table 2.

We restricted the model to cells for which forest cover was greater than zero in the year 2000, and to cells within the moist forest, dry forest and grassland biomes (cells without forest, or in the desert or mangrove biomes, were excluded).

We constructed a similar regression model for deforestation:

$$D_i = \exp(\beta_0^d + \beta_1^d AG_i + \mathbf{X}_i^d \beta_2^d + \mathbf{F}_i^d \beta_3^d + \gamma_i^d + \mu_i^d + \epsilon_i^d) \quad (2)$$

Here, the dependent variable, D_i , is the fraction of the area of cell i that underwent a forest to non-forest transition from 2000 to 2010. The independent

variables are the same as in the reforestation model in equation (1). The superscript *d* denotes deforestation.

We validated our pantropical grid-cell-level reforestation and deforestation models by comparing predicted and observed values at the country level from 2000 to 2010, obtaining a correlation coefficient of 0.95 for reforestation and 0.99 for deforestation. We also compared predicted values of country-level reforestation to the independent predictions of 76 country-specific models using the same functional form and variables, obtaining a correlation coefficient of 0.96 (the remaining 14 countries contained too few cells to run a country-specific regression model successfully). We did not validate our model using data from alternative time periods or datasets.

Projections of reforestation and deforestation under BAU. We projected future land-cover changes using a dynamic, recursive model from 2010 to 2050. For each future decade, *t* (2010–2020; 2020–2030; 2030–2040; 2040–2050), we calculated reforestation and deforestation in a cell as a function of cell attributes and the coefficients estimated in equations (1) and (2); that is:

$$\hat{R}_{it} = \epsilon(\hat{\beta}_0^r + \hat{\beta}_1^r AG_i + X_i^r \hat{\beta}_2^r + F_i^r \hat{\beta}_3^r + \hat{\gamma}_i^r + \hat{\mu}_i^r) \quad (3)$$

and

$$\hat{D}_{it} = \exp(\hat{\beta}_0^d + \hat{\beta}_1^d AG_i + X_i^d \hat{\beta}_2^d + F_i^d \hat{\beta}_3^d + \hat{\gamma}_i^d + \hat{\mu}_i^d) \quad (4)$$

Most cell attributes included in the model were time invariant, either in reality (slope, elevation, biome, continent) or by assumption (distance from cities, strict and multiple-use protected areas, potential agricultural revenue). Notably, we assumed that future real agricultural prices (2010–2050) would remain constant at average 2001–2010 levels, as suggested in ref. 48 for the period 2013–2022, and as used in ref. 12. We also assumed static yields, which may not be the case due to shifting agro-ecological conditions under climate change or due to agricultural intensification. We assumed that other unmodelled social, economic and political factors that affected the distribution of reforestation from 2000 to 2010 would remain static as well.

In contrast to other cell attributes, we updated forest cover dynamically; that is, we calculated forest cover at the end of each period by adding reforestation and subtracting deforestation during the previous period to the forest cover at the start of the period. We constrained forest cover such that the fraction of a cell that is forested could not decrease below zero or increase above one; that is:

$$F_{it+1} = \min\{\max[F_{it} - \hat{d}_{it} + \hat{r}_{it}, 0], 1\} \quad (5)$$

Projecting the behaviour of a system as complex and dynamic as tropical land cover to 2050, on the basis of 10 yr of data and a reduced-form model, is inherently challenging and inevitably involves simplifying assumptions. One of the greatest uncertainties involves how supply and demand for commodities will combine to affect future agricultural prices. We tested the sensitivity of our results to alternative assumptions that real agricultural prices would remain constant at lower or higher levels. Prices that were 50% lower resulted in a moderate (27%) rise in increased removals from reforestation at US\$20 tCO₂⁻¹, whereas prices that were 100% higher resulted in a large (41%) fall in increased removals from reforestation at US\$20 tCO₂⁻¹ relative to the base scenario using constant real agricultural prices.

Constructing CO₂ removal trajectories and emission factors. To convert the projections of reforestation into CO₂ removals, we constructed trajectories for how much carbon would be removed in each decade following reforestation. These trajectories (for example, ref. 49) varied based on two factors known to affect carbon accumulation: the biome in which reforestation took place and whether reforestation would be with plantation or natural forest.

We constructed a model of CO₂ removal over time in the aboveground biomass of growing forests that is based on a database of biomass stocks at 829 secondary tropical forest stands along with those stands' age, location and whether the forest was a plantation or natural regrowth¹⁵. We converted tonnes of biomass to tonnes of carbon stock by multiplying by 0.47 (ref. 50). We first tested which of four functional forms (that is linear; logarithmic; sigmoid; square root) best explained carbon stock as a function of age in a two-sided univariate regression. The square root of age explained a greater share of the variation in carbon stock than the alternatives. We then modelled the carbon stock in aboveground biomass of stand (*C_x^{AGB}*) as a function of the square root of the stand age (*A_x*); the square root of the stand age multiplied by a binary variable for forest type (*N_x*; 1 if a stand of forest was a plantation and 0 otherwise); and the square root of the stand age multiplied by binary variables for three biome types (*B_x*; moist forest, dry forest and reforestation within the grassland biome⁴³). The superscript *c* denotes carbon. We set the regression intercept to zero so that carbon stock was always zero, in year zero, by construction. We did not include an interaction term between plantation and biome type; that is:

$$C_x^{AGB} = \sqrt{A_x}(\beta_1^c + \beta_2^c N_x + \beta_3^c B_x) + \epsilon_x^c \quad (6)$$

This model explained 0.79 of variation in carbon stock across stands (see Supplementary Table 3; carbon stocks over time for different forest types are shown in Fig. 1 and Supplementary Fig. 1). For example, we estimated that a 20-year-old secondary natural forest in the moist tropical biome would have 51 t of aboveground carbon per hectare on average, which compares to others' estimates of 57 t of aboveground carbon per hectare on average for the neotropics⁵¹, and 26 t of aboveground carbon per hectare for natural regeneration following cultivation¹⁵.

Although we believe our estimates of carbon stock accumulation to be based on the best-fit curves to the best available dataset¹⁵, we were surprised not to find a larger difference in estimated sequestration rates between moist and dry tropical forests; for example, as found in ref. 51. Perhaps this has to do with biases in the location of stands included in the database from each biome. There is room for improvement with future research.

We next extrapolated across the tropics our model of how much carbon (tCha⁻¹) would be present in aboveground biomass in any cell, *i*, after *y* years of regrowth as forest type *n* (natural forest or plantation):

$$\hat{C}_{iyn}^{AGB} = \sqrt{y}(\hat{\beta}_1^c + \hat{\beta}_2^c N_i + \hat{\beta}_3^c B_i) \quad (7)$$

We assumed that historical average carbon accumulation rates would persist in future decades, which might not be the case if climate change affects carbon fertilization, soil moisture availability or fire frequency.

We calculated carbon stock in belowground biomass by applying a root-shoot ratio of 0.26 (ref. 52) to aboveground biomass:

$$\hat{C}_{iyn}^{BGB} = 0.26 \hat{C}_{iyn}^{AGB} \quad (8)$$

For plantation forests, we assumed a harvest-and-replanting cycle of 10 yr, which corresponds to typical rotation lengths for the most common tropical plantation species: eucalypts (7–10 yr), acacias (7–12 yr) and pines (10–30 yr)⁵³. In a sensitivity analysis we tested an alternative rotation length of 20 yr; this resulted in a small (5%) rise in increased removals from reforestation at US\$20 tCO₂⁻¹ relative to the base scenario using a 10 yr rotation length. For natural reforestation, we assumed no repeat clearing so carbon removal in secondary forests continued for decades. This is probably an overestimate because some amount of non-plantation regrowth is fallow that will be re-cleared for swidden (that is, 'slash and burn') agriculture (for example, ref. 54).

We modelled carbon stock in non-peat soils in cell *i*, after *y* years of regrowth as forest type *n* (*C_{iyn}^S*), by applying a linear regression with zero intercept to a database of soil carbon gained at tropical sites at varying years after a transition from non-forest to forest⁵⁵. Across 151 transitions to forest, the average carbon gain per year was 0.447% of pre-transition soil carbon. Across 150 transitions to plantation, the carbon gain per year was 0.919% of pre-transition soil carbon. We extrapolated soil carbon stocks across the tropics by applying these annual multipliers to the top 30 cm of soil carbon⁵⁶.

On peat soils, we did not include a carbon removal factor for soil as the GHG benefit is uncertain—carbon gains from rewetting and stopping further degradation may be counterbalanced by increased methane emissions from peatlands^{57–59}. We did not consider carbon stored in long-lived wood products in this analysis.

The total forest carbon stock in cell *i* in decade *t* as forest type *n* (*C_{itn}^{TOT}*) is the average forest carbon stock over the 10 yr of that decade, including in aboveground biomass, belowground biomass and non-peat soil:

$$\hat{C}_{itn}^{TOT} = \frac{1}{10} \sum_{y=10(t-1)}^{10t-1} \hat{C}_{iyn}^{AGB} + \hat{C}_{iyn}^{BGB} + \hat{C}_{iyn}^S \quad (9)$$

The carbon stock accumulation in the first decade of reforestation is equal to *C_{i1n}^{TOT}*, while the carbon stock accumulation in subsequent decades (that is during secondary forest regrowth) is equal to *C_{i2n}^{TOT} - C_{i1n}^{TOT}*, *C_{i3n}^{TOT} - C_{i2n}^{TOT}* and so on. We calculated the carbon removal factor (RF); that is, the amount of CO₂ removed from the atmosphere per hectare in cell *i*, in decade *t*, by forest type *n* (RF_{*itn*}), by multiplying the carbon stock accumulation by 3.67, the atomic ratio between CO₂ and carbon.

Finally, we allowed the carbon removal factor to vary by country to reflect the differential share of reforestation that occurs as natural forest rather than plantation:

$$RF_{itz} = \alpha_z RF_{it,natural} + (1 - \alpha_z) RF_{it,plantation} \quad (10)$$

That is, the CO₂ removed from the atmosphere per hectare at site *i*, in decade *t*, in country *z* (RF_{*itz*}) is a weighted average of the removal factors for natural forests (RF_{*it,natural*}) and plantations (RF_{*it,plantation*}), where α_z is the country-specific share of reforestation that is natural forest.

To make assumptions about the share of reforestation that would be natural forest regrowth versus plantation, we used data on the location of plantations¹⁶. These data were available for seven countries (Brazil, Cambodia, Colombia, Indonesia, Liberia, Malaysia and Peru), which together make up 45% of forest

cover in 2000, 34% of reforestation and 41% of deforestation from 2000 to 2010 among the countries in our sample, as well as 87% of global palm oil fruit production circa 2010³⁵. The location of plantation forests in these data was inferred on the basis of a visual interpretation by trained analysts of the geometric pattern of tree cover in 2013–2014 images. The dataset contained 296 plantation types, which we categorized into timber, oil palm or other (mostly fruit crops as well as young or unidentified plantations, see Supplementary Table 4). Overlays of plantation data and forest data showed that 3.6% of forest cover in 2010 and 15.2% of reforestation from 2000 to 2010 within these seven countries was identified as a plantation rather than natural forest regrowth. This fraction varied widely across these seven countries, from a low of 0.08% of forest cover and 0.14% of reforestation identified as a plantation in Peru, to a high of 27.2% of forest cover and 70.4% of reforestation identified as a plantation in Malaysia (Supplementary Table 4).

For the seven countries for which data on plantation coverage was available, we assumed that the fraction of future reforestation that would be plantation would be equal to the fraction of reforestation during 2000–2010 that was observed to be plantation in 2013–2014. For all of the other countries, we used the country from the same continent that had the lowest fraction of reforestation that was plantation (that is Peru for Latin America; Liberia for Africa; Cambodia for Asia), assuming that the countries for which plantation data were gathered were probably selected due to an above-average concentration of plantations. In sensitivity analyses, we tested alternative assumptions about the fraction of reforestation that was plantation (specifically, that the fraction of reforestation that would be plantation would be equal to the country with the median fraction of plantation from the same continent; that all reforestation would be plantation; and that all reforestation would be natural forest); these resulted in small to moderate (1–11%) differences in increased removals from reforestation at US\$20 tCO₂⁻¹ relative to the base scenario that extrapolated plantation area on the basis of continental minimums. Analyses such as ours would benefit from future research expanding maps of plantations from seven countries to the entire tropics or entire world.

For the CO₂ emission factors associated with deforestation, we used the same values as in ref. ¹²; that is, we assumed complete loss of aboveground and belowground biomass following deforestation. Aboveground biomass was taken from ref. ¹⁸, whereas belowground biomass was calculated by multiplying aboveground biomass by a root:shoot ratio of 0.26 (ref. ⁵²). On all peat soils (histosols and gleysols⁵⁰), we assumed soil emissions of 59.4 tCO₂ ha⁻¹ yr⁻¹ (ref. ⁶⁰) for 30 yr following deforestation, resulting in 1,782 tCO₂ ha⁻¹ of committed emissions. On non-peat soils we assumed soil emissions from deforestation to be 0.085 of soil carbon content in the top 30 cm (ref. ⁵⁶)—the unweighted pantropical average of the percentage of soil carbon released by conversion of forest to shifting cultivation and permanent crops or gained from conversion to pasture⁵⁵.

Projecting CO₂ removals and emissions under BAU. To calculate removals associated with the first decade of reforestation at site *i* (RR_{*i*}), we multiplied the area of reforestation in each cell by the CO₂ removed from the atmosphere by reforestation (tCO₂ ha⁻¹) in the first decade. To calculate removals associated with subsequent decades following reforestation (that is secondary forest growth) at site *i* (RR_{*i*}), we multiplied forest area gained in previous decades by removal factors for the second, third and so on decades. To calculate emissions from deforestation (ED) we multiplied the area deforested in a decade (for example, 2000–2010; 2010–2020; and so on) by the one-time emission factor (tCO₂ ha⁻¹).

We assumed that reforestation and deforestation would occur spatially independently within cells, such that net emissions from a cell are equal to the deforestation area multiplied by the emission factor minus the reforestation area times the removal factor. However, this is the upper bound for each gross flux. In a sensitivity analysis we assumed the maximum amount of spatial overlap between deforestation and reforestation (that is that deforestation and reforestation are of the same forest locations with the same carbon values), such that net emissions from a cell are equal to the net forest area change multiplied by the emission factor if net forest area change is negative or multiplied by the removal factor if the net forest area change is positive. This resulted in a moderate (19%) fall in increased removals from reforestation at US\$20 tCO₂⁻¹ relative to the base scenario in which areas of deforestation and reforestation did not overlap.

MAC curves. We next perturbed the BAU trajectory of reforestation by applying a per-hectare carbon price incentive effect (*C_i*) to equation (3), beginning in 2020. As in ref. ¹², a carbon price increased the return to standing forests relative to the potential to obtain agricultural revenue by converting forests to cropland or pasture, which increased expected reforestation. We calibrated the marginal effect of a carbon price on deforestation using the empirical relationship between the observed pattern of historical reforestation and deforestation and the variation across space and time in agricultural prices. We assumed that land users would respond equivalently to agricultural prices and carbon prices, as in the absence of evidence to the contrary, it is reasonable to assume equal price salience. In sensitivity analyses, we tested alternative assumptions that carbon prices would have lower or higher salience to land users. A 50%-lower price salience and a 100%-higher price salience resulted, respectively, in a large (51%) fall and a large

(108%) rise in increased removals from reforestation at US\$20 tCO₂⁻¹ relative to the base scenario with 1:1 price salience.

$$\hat{\mathbf{R}}_{it} = \exp(\hat{\beta}_0^r + \hat{\beta}_1^r (AG_i - C_i) + \mathbf{X}_i' \hat{\beta}_2^r + \mathbf{F}_i' \hat{\beta}_3^r + \hat{\gamma}_i^r + \hat{\mu}_i^r) \quad (11)$$

We assumed that a carbon pricing mechanism would pay for future carbon removals each year as they occur, and deduct for reversals from forest harvest as they occur, rather than pay for all carbon upfront. Land users would discount payments for removals farther in the future more heavily. Thus, the per-hectare incentive effect of a carbon price (US\$ ha⁻¹) on reforestation (*C_i*) is the carbon price (*P*) multiplied by the net present value of a stream of expected future payments for reforestation:

$$C_i = P \sum_{y=1}^{30} \text{RF}_{iy} \delta^y \quad (12)$$

RF_{*iy*} is the removal factor for cell *i* in year *y* (tCO₂ ha⁻¹ yr⁻¹), and δ is the discount rate. We applied a default discount rate of 10%, a rate that is typically used by development banks for evaluating public investments in developing countries³⁷, and that is consistent with private decision-making in the developing world³⁸. As mentioned above, in sensitivity analyses we applied an alternative 'ethical' discount rate of 3% (ref. ³⁸), an intermediate discount rate of 7% and a high discount rate of 15% to both future carbon payments and future agricultural revenues. We assumed that a carbon pricing mechanism would pay for up to thirty years of reforestation. In sensitivity analyses, we tested alternative payment lengths for reforestation of 50 or 100 yr, which resulted in small (2%) rises in increased removals from reforestation at US\$20 tCO₂⁻¹ relative to the base scenario. We assumed a frictionless translation of carbon price to land-user response. In sensitivity analyses, we tested the effects of implementation or transaction costs^{61,62} of US\$1,000 ha⁻¹, which resulted in moderate (36%) fall in removals from reforestation at US\$20 tCO₂⁻¹ relative to the base scenario with net costs equal to zero. We also tested the effects of co-benefits of US\$1,000 ha⁻¹, which resulted in a moderate (36%) increase in increased removals from reforestation at US\$20 tCO₂⁻¹ relative to the base scenario net costs equal to zero.

We assumed that increases in forest cover due to increased reforestation and decreased deforestation would not displace deforestation to new locations; that is, we assumed no 'leakage'. In a sensitivity analysis, we considered a scenario in which policy-induced increases in forest cover led to increases in agricultural prices, decreasing the likelihood of reforestation and increasing the likelihood of deforestation elsewhere, following the treatment of leakage in ref. ¹². This resulted in a small (10%) reduction in increased removals from reforestation at US\$20 tCO₂⁻¹ relative to the base scenario without leakage.

We traced out MAC curves for reforestation by projecting increased removals from reforestation at varying carbon prices. Increased removals from reforestation (IRR) at any given carbon price (*p*) was the difference between removals at that carbon price and removals under a BAU scenario:

$$\text{IRR}_{it,p} = \text{IRR}_{it,p} - \text{IRR}_{it,\text{BAU}} \quad (13)$$

Similarly to equation (11), we perturbed the BAU trajectory of deforestation by applying a per-hectare carbon price incentive effect (*C_i*) to the deforestation equation (4), beginning in 2020:

$$\hat{\mathbf{D}}_{it} = \exp(\hat{\beta}_0^d + \hat{\beta}_1^d (AG_i - C_i) + \mathbf{X}_i' \hat{\beta}_2^d + \mathbf{F}_i' \hat{\beta}_3^d + \hat{\gamma}_i^d + \hat{\mu}_i^d) \quad (14)$$

For deforestation, the per-hectare incentive effect of a carbon price (US\$ ha⁻¹) on deforestation was calculated by multiplying the carbon price (US\$ tCO₂⁻¹) by the emission factor (EF; tCO₂ ha⁻¹):

$$C_i = p \text{EF}_i \quad (15)$$

We traced out MAC curves for deforestation by projecting reduced emissions from deforestation at alternative carbon prices. Reduced emissions from deforestation (RED) at any given carbon price was the difference between emissions under a BAU trajectory and emissions at that carbon price:

$$\text{RED}_{it,p} = \text{ED}_{it,\text{BAU}} - \text{ED}_{it,p} \quad (16)$$

In calculating MAC curves for reforestation and deforestation, we modelled payments for reforestation and deforestation independently (that is, we kept one payment price at zero while varying the other payment price) to avoid complications arising from interactions between the two types of payments. In a sensitivity analysis, we allowed carbon prices to affect both reforestation and deforestation simultaneously; this resulted in a moderate (19%) fall in increased removals from reforestation at US\$20 tCO₂⁻¹ relative to the base scenario in which the two MACs were modelled separately.

We reported changes resulting from the imposition of carbon prices of US\$20 tCO₂⁻¹ and US\$50 tCO₂⁻¹ for consistency with past work. In European and

Californian carbon markets, US\$20tCO₂⁻¹ is roughly at the high end of current prices; US\$50tCO₂⁻¹ is roughly the global social cost of CO₂ emissions⁶³.

Caveats. We simulated the effects of a specific method for promoting reforestation—carbon payments. We did not model the cost per tonne of other methods that could be either less or more expensive, such as state-sponsored reforestation projects on public land, for example in China and India, which might not be as responsive to price signals. Our top-down estimates of the cost per tonne of reforestation across the entire tropics complement the range of bottom-up estimates of reforestation costs from specific countries and biomes, using specific policy levers, techniques and forest types (for example plantations, secondary natural forests, agroforests).

Our projections were based on observed patterns of reforestation and existing technologies during 2000–2010. For instance, although observed and projected reforestation within the grassland biome was mainly reforestation of woodland ecosystems, this probably also included some amount of forestation in native grasslands, a controversial activity with negative impacts on biodiversity^{26,64}. Promoting this activity further through carbon payments would violate safeguards related to biodiversity conservation.

Our model made no assumptions about potential growth in non-agricultural demand for alternate land uses; for example, BECCS. BECCS generated from annual crops would compete with reforestation for land area, whereas BECCS generated from forest biomass might encourage both reforestation and deforestation.

Reporting Summary. Further information on research design is available in the Nature Research Reporting Summary linked to this article.

Data availability

The data analysed in this study are available in the Harvard Dataverse repository (https://dataverse.harvard.edu/dataverse/tropical_reforestation_study).

Code availability

All code used during this study is available from the corresponding author on reasonable request.

References

- Busch, J. et al. Comparing climate and cost impacts of reference levels for reducing emissions from deforestation. *Environ. Res. Lett.* **4**, 044006 (2009).
- Busch, J. et al. Structuring economic incentives to reduce emissions from deforestation within Indonesia. *Proc. Natl Acad. Sci. USA* **109**, 1062–1067 (2012).
- Burivalova, Z. et al. Relevance of global forest change data set to local conservation: case study of forest degradation in masoala national park, Madagascar. *Biotropica* **47**, 267–274 (2015).
- Bellot, F. et al. *The high-resolution global map of 21st-century forest cover change from the University of Maryland ('Hansen Map') is hugely overestimating deforestation in Indonesia* (Forests and Climate Change Programme, 2014).
- Land Use, Land-use Change and Forestry* (UNFCCC, 2001).
- Global Agro-Ecological Zones (GAEZv 3.0)* (IIASA, FAO, 2012).
- FAOSTAT Database* (FAO, 2014).
- Naidoo, R. & Iwamura, T. Global-scale mapping of economic benefits from agricultural lands: implications for conservation priorities. *Biol. Conserv.* **140**, 40–49 (2007).
- Warusawitharana, M. *The Social Discount Rate in Developing Countries* (Federal Reserve, 2014); <https://doi.org/10.17016/2380-7172.0029>
- Lanza, A. et al. *Climate Change 2001: Mitigation* (eds Metz, B. et al.) Ch. 7 (IPCC, Cambridge Univ. Press, 2001).
- Jarvis A. et al. *Hole-Filled Seamless SRTM Data V4* (International Center for Tropical Agriculture, 2008).
- World Urbanization Prospects: The 2011 Revision* (UNDESA, 2012).
- World Database on Protected Areas* (World Conservation Monitoring Center, accessed 20 May 2014).
- Dinerstein, E. et al. An ecoregion-based approach to protecting half the terrestrial realm. *BioScience* **67**, 534–545 (2017).
- FAOSTAT: Forestry Production and Trade: Visualize Data* (FAO, 2018); <http://www.fao.org/faostat/en/#data/FO/visualize>
- Hughes, A. C. Have Indo-Malaysian forests reached the end of the road? *Biol. Conserv.* **223**, 129–137 (2018).
- Bowman, M. S. et al. Persistence of cattle ranching in the Brazilian Amazon: a spatial analysis of the rationale for beef production. *Land Use Policy* **29**, 558–568 (2012).
- Wooldridge, J. M. *Econometric Analysis of Cross Section and Panel Data* (MIT Press, 2002).
- Burgess, R., Hansen, M., Olken, B. A., Potapov, P. & Sieber, S. The political economy of deforestation in the tropics. *Q. J. Econ.* **127**, 1707–1754 (2012).
- OECD-FAO Agricultural Outlook 2013–2022* (Organisation for Economic Co-operation and Development, FAO, 2013).
- Bonner, M. T. L., Schmidt, S. & Shoo, L. P. A meta-analytical global comparison of aboveground biomass accumulation between tropical secondary forests and monoculture plantations. *For. Ecol. Manag.* **291**, 73–80 (2013).
- IPCC 2006 IPCC Revised Guidelines for National Greenhouse Gas Inventory* (Cambridge Univ. Press, 2006).
- Poorter, L. et al. Biomass resilience of Neotropical secondary forests. *Nature* **530**, 211–214 (2016).
- Mokany, K. et al. Critical analysis of root:shoot ratios in terrestrial biomes. *Glob. Change Biol.* **12**, 84–96 (2006).
- Ugalde, L. & Perez, O. *Mean Annual Volume Increment of Selected Industrial Forest Plantation Species* (FAO, 2001).
- Schwartz, N. B., Uriarte, M., DeFries, R., Gutierrez-Velez, V. H. & Pinedo-Vasquez, M. A. Land-use dynamics influence estimates of carbon sequestration potential in tropical second-growth forest. *Environ. Res. Lett.* **12**, 074023 (2017).
- Powers, J. S., Corre, M. D., Twine, T. E. & Veldkamp, E. Geographic bias of field observations of soil carbon stocks with tropical land-use changes precludes spatial extrapolation. *Proc. Natl Acad. Sci. USA* **108**, 6318–6322 (2011).
- Harmonized World Soil Database (Version 1.0)* (FAO/IIASA/ISRIC/ISSCAS/JRC, 2008).
- Mitsch, W. J. et al. Wetlands, carbon, and climate change. *Landsc. Ecol.* **28**, 583–597 (2013).
- Bridgman, S. D., Moore, T. R., Richardson, C. J. & Roulet, N. T. Errors in greenhouse forcing and soil carbon sequestration estimates in freshwater wetlands: a comment on Mitsch et al. (2013). *Landsc. Ecol.* **29**, 1481–1485 (2014).
- Neubauer, S. C. On the challenges of modeling the net radiative forcing of wetlands: reconsidering Mitsch et al. (2013). *Landsc. Ecol.* **29**, 571–577 (2014).
- Murdiyarso, D. et al. Opportunities for reducing greenhouse gas emissions in tropical peatlands. *Proc. Natl Acad. Sci. USA* **107**, 19655–19660 (2010).
- Torres, A. B., Marchant, R., Lovett, J. C., Smart, J. C. R. & Tipper, R. Analysis of the carbon sequestration costs of afforestation and reforestation agroforestry practices and the use of cost curves to evaluate their potential for implementation of climate change mitigation. *Ecol. Econ.* **69**, 469–477 (2010).
- Galik, C. S., Cooley, D. M. & Baker, J. S. Analysis of the production and transaction costs of forest carbon offset projects in the USA. *J. Environ. Manag.* **112**, 128–136 (2012).
- Technical Support Document: Technical Update of the Social Cost of Carbon for Regulatory Impact Analysis Under Executive Order 12866* (United States Government, 2016).
- Bond, W. J. Ancient grasslands at risk. *Science* **351**, 120–122 (2016).